

Si-96-13

# Generalized Dynamic Scaling for Critical Magnetic Systems

B. Zheng

Universität – GH Siegen, D – 57068 Siegen, Germany

## Abstract

The short-time behaviour of the critical dynamics for magnetic systems is investigated with Monte Carlo methods. Without losing the generality, we consider the relaxation process for the two dimensional Ising and Potts model starting from an initial state with very high temperature and arbitrary magnetization. We confirm the generalized scaling form and observe that the critical characteristic functions of the initial magnetization for the Ising and the Potts model are quite different.

PACS: 75.10.-b, 64.60.Ht, 02.70.Lq, 05.50.+q

# 1 Introduction

The critical phenomena for magnetic systems in the equilibrium have long been studied. Due to the large correlation length near the critical point, the large scale behaviour of the systems does not depend on the microscopic details. An universal scaling form characterized by a number of critical exponents describes the scale invariance in critical systems. For magnetic systems in *a non-equilibrium state*, however, it is much less understood. Indeed, for dynamic systems in *the long time regime* where the equilibrium is almost reached, one finds also a dynamic scaling form. Due to critical slowing down, however, numerical study of critical dynamics is very difficult. Even for the simplest system as the two-dimensional Ising model, the dynamic exponent  $z$  has not rigorously been determined. Even though much effort has been put to develop fast algorithms to overcome critical slowing down, the dynamic scaling has not yet been deeply investigated.

Recently a dramatic step forward in the study of critical dynamics has been made. For a relaxation process starting from an initial state with *very high temperature and small magnetization*, it is argued that universal scaling behaviour already emerges in *the macroscopic early time* [1, 2, 3, 4]. Important is that another dynamic exponent should be introduced to describe the dependence of the scaling behaviour on the initial magnetization. It has also been discussed that under certain conditions the effect of the initial magnetization remains even in the long-time regime of the critical relaxation [5, 6]. Numerical simulations support these predictions [7, 8, 9, 10, 11, 12, 13, 14, 15]. In the equilibrium state, introducing the lattice size  $L$  as a scaling variable in the finite size scaling induces essential progress in the study of critical phenomana, especially in the numerical simulation. In dynamic systems, besides the lattice size  $L$  we now have the evolution time  $t$  as another scaling variable. Different from the case in the long time regime, it is demonstrated that in short-time dynamics the scaling variable  $t$  plays a very important role in understanding the scaling behaviour, especially in numerical simulations. The critical exponents can be obtained from the power law behaviour of the observables in the early time  $t$  [10, 12, 16, 17] or from the time-dependent finite size scaling [18, 19]. Numerical results indicate that the study of short-time dynamics not only enlarges the fundamental knowledge on critical phenomena but also provides new ways to determine all the static as well as the dynamic exponents.

For the understanding of the universal behaviour in short-time dynamics, we should keep in mind that there exist two completely different time scales, *the macroscopic time scale and the microscopic time scale*. Universal behaviour emerges only after a time period which is long enough in the microscopic sense. This time period is called the microscopic time scale  $t_{mic}$ . We expect that  $t_{mic}$  would be very small compared with the macroscopic time scale which is typically  $t_{mac} \sim L^z$  or  $t_{mac} \sim \tau^{-\nu z}$ . Here  $z$  is the dynamic exponent and  $\tau$  is the reduced temperature. However, how big  $t_{mic}$  is depends on the microscopic de-

tails. If  $t_{mic}$  would be so big as comparable with the macroscopic time scale  $t_{mac}$ , what one claims for the universal behaviour in the short-time dynamics becomes meaningless.

In Ref. [12, 17], the short-time behaviour of the critical dynamics for the two dimensional Ising and Potts model has carefully and seriously been analysed. Simulations have been performed with both the heat-bath and the Metropolis algorithm. Fortunately, it is discovered that  $t_{mic} \sim 5 - 30$  Monte Carlo time steps for both algorithms. If one thinks a Monte Carlo time step is a typical microscopic time unit, this result is quite reasonable. Taking into account the possible effect of  $t_{mic}$ , critical exponents  $\theta$ ,  $z$  and  $\beta/\nu$  are confidently obtained for both algorithms [12, 17]. The results are well consistent and strongly support universality in the short-time dynamics. Interestingly, when the dynamic system exhibits already universal behaviour in the macroscopic short-time regime, the spatial correlation length is still not so big, e.g. for the Potts model at  $t = 100$ ,  $\xi \sim 5$  [10]. Some more discussions on universality in short-time dynamics may also be found in the recent preprints [14, 20, 21, 22].

Does the critical exponent  $\theta$  (or  $x_0$ ) describe all the new physics in short-time dynamic systems? Very recently, it has been suggested that due to the fact that the time evolution of the magnetization is *not a Markovian process*, the global persistence exponent is also an independent critical exponent in the dynamic systems [23, 24]. Numerical simulations show that this is indeed the case [23, 20]. The power law decay of the global persistence probability is directly observed and the global persistence exponent for the two dimensional Ising and Potts model is determined to a satisfactory accuracy [20].

Since the scenario described above is so attractive and, on the other hand, all the results indicate that we are still far from a complete understanding of the critical short-time dynamics, we would like to push forward the study of more general dynamic processes. In a previous letter [25], the author has numerically investigated the short-time behaviour of the critical relaxation for the two dimensional Potts model starting from an initial state with *very high temperature and arbitrary magnetization*. A generalized dynamic scaling is found to describe the crossover behaviour for the short-time dynamics from the repulsive fixed point  $m_0 = 0$  to the attractive fixed point  $m_0 = 1$ . The critical characteristic function for the initial magnetization is numerically determined from the finite size scaling.

The present paper is an extension of the previous letter. We aim to present a systematic description of the numerical data, and meanwhile pay attention to the microscopic time scale  $t_{mic}$ . Compared with the data reported in the previous letter, the maximum evolution time  $t$  here is extended to  $t = 2000$  for the lattice size  $L = 144$  and  $t = 400$  for the lattice size  $L = 72$ , twice as long as in the previous letter [25]. This allows us to see how stable the results are with respect to the time  $t$ . To reduce the fluctuations, we have also increased the statistics for the lattice size  $L = 144$  for the bigger initial magnetization  $m_0$ . Furthermore, as

an alternative example, we have carried out also a similar simulation for the two dimensional Ising model. We interestingly observe that the critical characteristic functions for the initial magnetization for these two models are quite different. Finally some discussions are given corresponding to a recent preprint on this topic [26].

In the next section, we present scaling analyses for the short-time dynamics based on which the numerical data will be analysed. In Sec. 3, numerical results for the two dimensional Potts and Ising model will be reported. The last section contains the conclusions.

## 2 Scaling analysis

For the critical relaxation process of a dynamics of the Model A starting from an initial state with *very high temperature* and *small magnetization*, Janssen, Schaub and Schmittmann [1] proposed a dynamic scaling form which is valid up to the macroscopic short-time regime,

$$M^{(k)}(t, \tau, m_0) = b^{-k\beta/\nu} M^{(k)}(b^{-z}t, b^{1/\nu}\tau, b^{x_0}m_0) \quad (1)$$

where  $M^{(k)}$  is the  $k$ -th moment of the magnetization,  $t$  is the dynamic evolution time,  $\tau$  is the reduced temperature, and the parameter  $b$  represents the spatial rescaling factor. Besides the well known static critical exponents  $\beta$ ,  $\nu$  and the dynamic exponent  $z$ , a new independent exponent  $x_0$  which is the anomalous dimension of the initial magnetization  $m_0$  is introduced to describe the dependence of the scaling behaviour on the initial magnetizations. Based on the scaling relation it is predicted that at the beginning of the time evolution the magnetization surprisingly undergoes a *critical initial increase*

$$M(t) \sim m_0 t^\theta \quad (2)$$

where the exponent  $\theta$  is related to the exponent  $x_0$  by  $\theta = (x_0 - \beta/\nu)/z$ .

The scaling form in Eq. (1) is valid only under the conditions that the initial state is at very high temperature with *small* initial magnetization. For a critical relaxation from an initial state with very high temperature and *arbitrary magnetization*, is there universal scaling behaviour in the short-time regime?

In Fig. 1, time-dependent magnetization profiles with different initial magnetizations  $m_0$  for the critical Potts model are displayed. The lattice size is  $L = 72$ . For smaller  $m_0$ , the magnetization continuously increases. The time scale for this increase is  $t_0 \sim m_0^{-z/x_0}$ . For bigger  $m_0$ , the magnetization rises up rapidly and then decreases. After a macroscopic long time  $t_{mac} \sim L^z$  (out of the time range of Fig. 1), we expect that all the profiles gradually join together and decrease exponentially. Traditionally, when we consider the dynamic scaling in the long-time regime the effect of the initial conditions is always neglected. However, as we can

see in Fig. 1, in the short-time regime the effect of the initial magnetization is very prominent, which is more or less due to the fact the exponent  $\theta$  is positive. Therefore it is important and interesting to study whether there exists universal behaviour in the short-time dynamics.

A scaling form represents nothing else than a kind of scale invariance, or self-similarity in the systems. At the critical point the time correlation length of the dynamic systems is infinity, therefore we may expect a certain scale invariance independent of the initial conditions. The self-similarity of the magnetization profiles for different  $m_0$  may also be observed in Fig. 1. Important is that we should consider the scaling behaviour of the initial magnetization carefully. In the previous letter [25], the author proposed a generalized dynamic scaling form, e.g. for the  $k$ -th moment of the magnetization,

$$M^{(k)}(t, \tau, L, m_0) = b^{-k\beta/\nu} M^{(k)}(b^{-z}t, b^{1/\nu}\tau, b^{-1}L, \varphi(b, m_0)) \quad (3)$$

For the convenience of later discussions, finite systems have been considered here and  $L$  is the lattice size. The scaling behaviour of the initial magnetization  $m_0$  is specified by the critical characteristic function  $\varphi(b, m_0)$ , which in the limit  $m_0 \rightarrow 0$  tends to the simple form  $b^{x_0}m_0$  used in Eq.(1), but is in general different. To avoid possible confusion, we have changed the notation  $\chi$  for the critical characteristic function in the previous letter to  $\varphi$  in this paper. This generalized scaling form describes the crossover behaviour between two fixed points, the repulsive one  $m_0 = 0$  and the attractive one  $m_0 = 1$ . It is also in a similar spirit as that in the correction to the scaling, where non-linear effects of an off-fixed point are considered. In general cases of the crossover phenomena, however,  $m_0$  would also enter the scaling behaviour of the time  $t, \tau$  and the anomalous dimension of  $M^{(k)}$ , or the exponents  $z, \beta$  and  $\nu$  would depend on  $m_0$ . Then the situation will be very complicated and numerical simulations are difficult.

The simple ansatz of the scaling form in Eq.(3) for the short-time dynamics that the exponents  $\beta, \nu$  and  $z$  do not depend on the initial magnetization  $m_0$  is based on the fact that if we believe there is a scaling form in the short-time regime of the dynamic relaxation process, this scaling form should smoothly cross over to that in the long-time regime. In other words, the initial magnetization should not enter the renormalization of the critical system in equilibrium and near equilibrium. However, the dimension of the initial magnetization would, in general, depend on the value of the initial magnetization. Assuming that we can either perturbatively or non-perturbatively perform the renormalization calculation of the dynamic system, the renormalization equation for the initial magnetization  $m_0$  may be written as

$$\frac{\partial \ln m(\lambda)}{\partial \ln \lambda} = \eta_0(m(\lambda)). \quad (4)$$

Here  $\eta_0(m(\lambda))$  is the anomalous dimension of the initial magnetization and all the irrelevant operators are already set to the fixed points. The solution of the

equation (4) gives the critical characteristic function  $\varphi(b, m_0)$ . Therefore  $\varphi(b, m_0)$  can be written in a form

$$\varphi(b, m_0) = F(bF^{-1}(m_0)) \quad (5)$$

with condition  $\varphi(1, m_0) = m_0$ . If we define  $g = F^{-1}(m_0)$ , under the renormalization group transformation  $g$  will be scaled as  $bg$ . Then we may conclude that the time scale where the effect of  $m_0$  remains is  $g^{-z}$ .

We should also point out that the dynamic scaling form in Eq.(3) may straightforwardly be generalized to a critical relaxation process starting from an initial state with an *arbitrary temperature* and arbitrary magnetization. In general the initial temperature will also enter the dimension of the initial magnetization and vice versa. The critical characteristic functions for the initial magnetization and temperature are a bit more complicated.

In order to verify the scaling form in Eq.(3), as a first approach, in this paper we always set  $\tau = 0$ . We perform simulations for a pair of lattice sizes  $L_1$  and  $L_2$ . From the scaling collapse of the magnetization or its higher moments, in principle, we can estimate the values of the function  $\varphi(b, m_0)$  at  $b = L_2/L_1$  for different  $m_0$ . This works always well in case of smaller initial magnetization. When the initial magnetization  $m_0$  is bigger, the dynamic system leaves the repulsive fixed point  $m_0 = 0$  and approaches to the attractive fixed point  $m_0 = 1$ . The determination of the function  $\varphi(b, m_0)$  becomes more difficult since the dependence of the observables on the initial magnetization gets weaker. To reduce the extra fluctuations from  $M^{(k)}(t, 1)$ , we may introduce a magnetization difference

$$M_d(t, m_0) = M^{(1)}(t, 1) - M^{(1)}(t, m_0) \quad (6)$$

and a Binder-type cumulant

$$U_d(t, m_0) = \frac{M^{(2)}(t, 1) - M^{(2)}(t, m_0)}{[M_d(t, m_0)]^2} \quad (7)$$

to measure the function  $\varphi(b, m_0)$ .

### 3 Generalized dynamic scaling

In this section, we present numerical results for the short-time dynamics of the two-dimensional 3-state Potts and Ising model. In the first subsection, we systematically analyse the data for the Potts model and demonstrate how to determine the critical characteristic function  $\varphi(b, m_0)$  from the finite size scaling. In the second subsection, we report the results for the Ising model and meanwhile discuss some relevant important problems.

In this section, all the simulations and discussions are restricted to the case  $\tau = 0$ , i.e. the dynamic system is exactly at the critical point. Therefore the exponent  $\nu$  will not enter the calculation.

### 3.1 The Potts model

The Hamiltonian for the  $q$ -state Potts model is given by

$$H = K \sum_{\langle ij \rangle} \delta_{\sigma_i, \sigma_j}, \quad \sigma_i = 1, \dots, q \quad (8)$$

where  $\langle ij \rangle$  represents nearest neighbours. In our notation the inverse temperature is already absorbed into the coupling  $K$ . It is known that the critical points locate at  $K_c = \log(1 + \sqrt{q})$ . In this paper the 3-state case will be investigated. The exact value of the static exponents  $\beta/\nu = 2/15$  and the dynamic exponent  $z = 2.196(8)$  obtained from the power law decay of the auto-correlations [10, 12] will be taken as input. In the numerical simulations, we measure the  $k$ th moment defined as

$$M^{(k)}(t, m_0) = \left\langle \left[ \frac{3}{2N} \sum_i (\delta_{\sigma_i(t), 1} - \frac{1}{3}) \right]^k \right\rangle, \quad (9)$$

where the average is taken over independent initial configurations and the random forces. The initial magnetization  $m_0$  has sharply been prepared.

In order to determine the critical characteristic function  $\varphi(b, m_0)$ , in the previous letter we have performed the simulation for different lattice sizes,  $L = 36, 72$  and  $144$  with samples of different initial configurations 80 000, 40 000 and 8 000 respectively. For the initial magnetization  $m_0$ , we take the value  $m_0 = 0.14, 0.22, 0.30, 0.40, 0.50, 0.60, 0.70, 0.80$  and  $1.00$  for the lattice size  $L = 144$ . For  $m_0 \geq 0.50$ , the data are more fluctuating and therefore in this paper we increase the statistics for the lattice size  $L = 144$  to 16 000 and for the lattice size  $L = 72$  to 80 000. We updated the dynamic system to the maximum evolution time  $t = 2000$  for the lattice size  $L = 144$ ,  $t = 500$  for the lattice size  $L = 72$  and  $t = 100$  for the lattice size  $L = 36$ . From the scaling collapse of an observable for two different lattice sizes  $L_1$  and  $L_2$  with suitable initial magnetizations, we can estimate the values of the function  $\varphi(b, m_0)$  at  $b = L_2/L_1$  for different  $m_0$ . In principle, any observables which essentially depend on the initial magnetization may be used for this purpose. In this paper, the statistical errors are estimated by dividing the samples with different initial configurations into four groups.

In Fig. 2a, the scaling plot for the magnetization is displayed for the lattice  $L_1 = 72$  and the lattice  $L_2 = 144$ . The initial magnetization for the lattice  $L_2 = 144$  is  $m_{02} = 0.14$ . If one can find an initial magnetization  $m_{01}$  for lattice  $L_1 = 72$  such that the time evolution curves of the magnetizations for both lattice sizes collapse, the scaling is valid and from the scaling form in Eq.(3) one gets  $\varphi(2, m_{02}) = m_{01}$ . In Fig. 2a, stars represent the time evolution of the magnetization of the lattice  $L_2 = 144$ . Crosses are the same data but rescaled in time and multiplied by an overall factor  $2^{\beta/\nu}$ . For the lattice  $L_1 = 72$ , we have performed the simulation with two different initial magnetizations  $m_0 = 0.175$  and  $m_0 = 0.185$ , for which the magnetizations have been plotted by the lower

and upper solid lines. By linear extrapolation, we obtain the time evolution of the magnetization with initial values between these two values. The solid line laying on the crosses in Fig. 2a is the time evolution of the magnetization for  $L = 72$  with an initial magnetization  $m_{01} = 0.1802(6)$  which has the best fit to the crosses. Therefore,  $\varphi(2, 0.14) = 0.1802(6)$ . Compared with the scaling plot for the magnetization difference  $M_d(t, m_0)$  presented in Fig. 1 in the previous letter, the evolution time has been extended to  $t = 400$  in the time scale of the lattice size  $L = 72$ . The quality of the fit in Fig. 2a is as good as that in Fig. 1 in the previous letter. The resulting value for  $\varphi(2, 0.14) = 0.1802(6)$  is also very well consistent with  $\varphi(2, 0.14) = 0.1800(4)$  in the previous letter [25].

However, when the initial magnetization  $m_0$  is getting bigger, the determination of the function  $\varphi(b, m_0)$  becomes more and more difficult since the dependence of the observables on  $m_0$  is weakening. For example, the time dependent magnetization  $M(t, m_0)$  can be written as  $M(t, m_0) = M_d(t, m_0) + M(t, 1)$ . The part depending on  $m_0$  is only  $M_d(t, m_0)$ . For relative big  $m_0$ , e.g.  $m_0 \geq 0.50$ ,  $M_d(t, m_0)$  is much smaller than  $M(t, 1)$ . Therefore a small relative error of  $M(t, 1)$  may induce bigger errors for the function  $\varphi(b, m_0)$  when it is determined from the scaling plot of  $M(t, m_0)$ . In Fig. 2b, such a situation is shown for a scaling plot for  $L = 144$  with  $m_0 = 0.50$ . The quality of the scaling collapse is not so good.

The errors of  $M(t, 1)$  have many origins. There are apparently statistical errors. In the rescaling of  $M(t, m_0)$ , the error of the dynamic critical exponent  $z$  also enters. More important is the effect of the microscopic time scale  $t_{mic}$ . As it is discussed in the numerical measurements of the critical exponent  $\theta$  in Ref [12, 16],  $t_{mic}$  becomes bigger as the initial magnetization  $m_0$  increases. For  $M(t, m_0 = 1)$ , it is observed that  $t_{mic} \sim 50$  [16]. Finally, the systematic errors of the random numbers might also play some role.

As pointed out in the previous letter, to reduce the extra errors from  $M(t, 1)$  one can directly estimate the function  $\varphi(b, m_0)$  from the scaling collapse of  $M_d(t, m_0)$ . In Fig. 3, a scaling plot of  $M_d(t, m_0)$  for lattice size  $L = 144$  with  $m_0 = 0.50$  and lattice size  $L = 72$  is plotted. Now, the fitting of the data is much better than that for  $M(t, m_0)$ . The crosses lie nicely on the fitted solid line in the whole time interval. As it will carefully be discussed below, the microscopic time scale  $t_{mic}$  shows to be quite small here. The resulting value of  $\varphi(b, m_0)$  is  $\varphi(2, 0.50) = 0.6586(31)$ .

In any case, errors induced by the error of the exponent  $z$  still remain for the scaling plot of  $M_d(t, m_0)$ . In the above estimation of the values for the function  $\varphi(b, m_0)$ , these errors have not been taken into account. For this reason, we have performed the scaling fitting with two different values of  $z$ ,  $z = 2.176$  and  $z = 2.216$ . The results for  $\varphi(2, 0.50)$  are  $\varphi(2, 0.50) = 0.6571(29)$  and  $\varphi(2, 0.50) = 0.6602(30)$  respectively. Compared with the value obtained with  $z = 2.196$ , the difference is not big. Actually all the values are covered by the statistical errors. In contrast to this, the result for the exponent  $z$  given in Ref [12] is  $z = 2.196(8)$  and the statistical error is already negligible.

In order to reveal the fine struture of the short-time behaviour of the critical dynamics, we can proceed in a different way to measure the critical characteristic function  $\varphi(b, m_0)$ . Especially we would like to pay attention to the possible effect of the microscopic time scale  $t_{mic}$  discussed in Sec. 1, and see also how stable the scaling form in Eq.(3) is with respect to the evolution time. Theoretically, the scaling form in Eq.(3) is valid for every time  $t$  after the microscopic time scale  $t_{mic}$ . In Fig. 3, the function  $\varphi(b, m_0)$  is determined by searching for the best fit of the data in a time interval [10, 400]. We may call this ‘*global*’ fit. Actually, the function  $\varphi(b, m_0)$  can be estimated from the data in any ‘local’ time  $t$ . For example, we can perform the fitting at a time  $t$  in the time interval  $[t, t + 15]$  and measure the function  $\varphi(b, m_0)$ . We may call this ‘*local*’ fit.

In Fig. 4a, 4b and 4c, the resulting function  $\varphi(2, m_0)$  from the magnetization difference  $M_d(t, m_0)$  for the lattice size  $L = 144$  and  $L = 72$  as a function of the time  $t$  is plotted for the initial magnetization  $m_0 = 0.14, 0.30$  and  $0.60$ . The errors are estimated by dividing the samples with different initial configurations into four groups. Taking into account the errors, from the figures we see that  $\varphi(2, m_0)$  as a function of time  $t$  fluctuates around a constant value after a microscopic time scale  $t_{mic} \leq 10$ . This is a strong indication that the scaling form in Eq.(3) is valid. Such a small  $t_{mic}$  is consistent with what we observe in the numerical measurement of the critical exponent  $\theta$  [12]. The final value of  $\varphi(2, m_0)$  can be estimated by taking the average over a certain time interval. For example, for  $m_0 = 0.14$  we obtain  $\varphi(2, 0.14) = 0.1801(6)$  by averaging over time interval [10, 400]. This coincides well with that obtained from the ‘*global*’ fit. From Fig. 4a, 4b and 4c, we can also see the tendency that the fluctuations become bigger as  $m_0$  increases. For  $m_0 = 0.14$  the fluctuations are around one percent but for  $m_0 = 0.60$  those are already around five percent.

Here we should stress that the data points of the function  $\varphi(2, m_0)$  at different time  $t$  presented in Fig. 4a, 4b and 4c are not completely statistically independent. The data points within a time distance of 15 are obtained from time intervals which partly overlap each other. Even for the data points with a time distance bigger than 15, they are in some way correlated due to the large time correlation length. Therefore, using the data in Fig.4a, 4b and 4c to estimate the statistical errors is complicated. For these reasons, our statistical errors are always estimated by dividing the samples with different initial configurations into four groups. However, we should also keep in mind that the data points presented in Fig. 4a, 4b and 4c are also not completely statistically dependent. How these data points correlate in the time direction just represents the characteristic property of the time evolution of the magnetization. This kind of pictures as Fig.4a, 4b and 4c have shown to be useful in handling the possible effects of the microscopic time scale  $t_{mic}$  and of finite lattice sizes [19, 12]. It helps us to decide in which time interval we should perform the ‘*global*’ fit to obtain the final results for the function  $\varphi(b, m_0)$ .

The function  $\varphi(b, m_0)$  can also be obtain from other observables. In Fig.5, a

scaling plot is shown for the Binder-type cumulant  $U_d(t, m_0)$  for the lattice size  $L = 144$  with  $m_0 = 0.14$  and the lattice size  $L = 72$ . The result  $\varphi(2, 0.14) = 0.1795(8)$  is as good as that estimated from  $M_d(t, m_0)$ . To determine the function  $\varphi(b, m_0)$  from the cumulant  $U_d(t, m_0)$ , one does not need the static exponent  $\beta/\nu$  as an input. This is an advantage. The fact that  $\varphi(b, m_0)$  obtained from both  $M_d(t, m_0)$  and  $U_d(t, m_0)$  coincide well provides strong support for the generalized scaling form in Eq.(3). However, for bigger initial magnetization, e.g.  $m_0 \geq 0.50$ ,  $U_d(t, m_0)$  fluctuates much more than  $M_d(t, m_0)$  does.

In Table 1, the functions  $\varphi(2, m_0)$  and  $\varphi(4, m_0)$  obtained from a global fit of the magnetization difference  $M_d(t, m_0)$  are listed. To estimate  $\varphi(2, m_0)$ , the fitting is carried out in a time interval [10, 200] for smaller  $m_0$ , while in a time interval [10, 100] for  $m_0 > 0.50$ . For  $\varphi(4, m_0)$  the fitting is performed in a time interval [10, 100] for smaller  $m_0$ , while in a time interval [10, 50] for  $m_0 > 0.50$ . The errors are estimated by dividing the samples with different initial configurations into four groups. Compared with the data in the previous letter the results for bigger  $m_0$  are improved.

In order to get a more direct understanding of the full critical characteristic function  $\varphi(b, m_0)$ , in the previous letter we have defined an effective dimension  $x(b, m_0)$  of the initial magnetization  $m_0$  by  $\varphi(b, m_0) = b^{x(b, m_0)} m_0$ . Taking the results from Table 1, the corresponding effective dimensions  $x(b, m_0)$  are plotted in Fig. 6. Circles are of  $x(2, m_0)$  and crosses are of  $x(4, m_0)$ . They clearly show that the function  $\varphi(b, m_0)$  is not a constant with respect to  $m_0$ . Later we will come back to this point at the end of the next subsection.

Before closing this subsection, we would like to discuss on the technique of *the sharp preparation of the initial magnetization* in the numerical simulations. Taking the Potts model as an example, we randomly generate the initial spin configurations such that each spin takes value +1 with probability  $(1 + 2m_0)/3$ , while 0 and -1 with probability  $(1 - m_0)/3$ . If the lattice size is infinite, a *sharp* value  $m_0$  for the initial magnetization is automatically achieved. However, practically our lattice size is finite. Then the initial magnetization obtained in this way fluctuates around the value  $m_0$ , depending on the lattice size  $L$ . This is an extra kind of finite size effects. To reduce this effect, we usually adopt the sharp preparation technique: when the initial magnetization does not take the value  $m_0$ , we randomly select a spin on the lattice and flip it if the updated magnetization comes nearer to  $m_0$ ; we continue this procedure until the initial magnetization reaches the value  $m_0$ . In the previous numerical simulations, this technique has been widely used and shown its efficiency. [9, 10, 16, 18, 19, 27]. For sufficient big lattice sizes, whether one applies the sharp preparation technique does not make a big difference, but the data with sharply prepared  $m_0$  show in general less extra finite size effects. How important the sharp preparation technique is depends also on the initial magnetization  $m_0$  and what kind of observables one measures. The smaller (or nearer to one) the initial magnetization  $m_0$  is, the more important sharp preparation technique becomes. In two very recent preprints [14, 20], more

detailed discussions on this problem have been presented. A typical example is the measurement of the global persistence exponent [23, 20]. Without the sharp preparation technique, it is very difficult to observe the power law decay of the persistence probability of the (global) magnetization and the extra finite size effect remains even when the lattice size  $L = 256$  for the two dimensional Ising model [20].

For the measurement of the critical characteristic function, we have also repeated some calculations without the sharp preparation of the initial magnetization. In Fig. 7, a scaling plot for the magnetization difference  $M_d(t)$  is displayed for the lattice size  $L = 72$  and  $L = 144$ . The initial magnetization for  $L = 144$  is  $m_0 = 0.14$ . Stars represent the time evolution of the magnetization difference for  $L = 144$ , while the lower and upper solid line are those for  $L = 72$  with  $m_0 = 0.175$  and  $m_0 = 0.185$  respectively. For comparison, the corresponding magnetizations for the lattice size  $L = 144$  and  $L = 72$  with the sharp preparation of the initial magnetization have also been displayed by the dotted line and the dashed lines in the figure. We see the difference between with and without the sharp preparation technique is already not big. The crosses are the same data as the stars but rescaled in time. The resulting value of  $\varphi(b, m_0)$  is  $\varphi(2, 0.14) = 0.1811(9)$ . Within the statistical errors, this is consistent with  $\varphi(2, 0.14) = 0.1800(4)$  obtained with the sharp preparation technique. Similarly, without the sharp preparation technique we obtain  $\varphi(2, 0.40) = 0.5283(17)$ . Looking at Table 1, all these results show that for the lattice as big as  $L = 72$  and  $L = 144$  the difference between with and without the sharp preparation technique is within the statistical errors.

### 3.2 The Ising model

The Hamiltonian for the Ising model is

$$H = J \sum_{\langle ij \rangle} S_i S_j , \quad S_i = \pm 1 , \quad (10)$$

with  $\langle ij \rangle$  representing nearest neighbours. In equilibrium the Ising model is exactly solvable. The critical point locates at  $J_c = \log(1 + \sqrt{2})/2$  and the exponent  $\beta/\nu = 1/8$ . The  $k$ th moment is defined as

$$M(t) = \left\langle \left[ \frac{1}{N} \left\langle \sum_i S_i(t) \right\rangle \right]^k \right\rangle . \quad (11)$$

In this section, we follow the same procedure as demonstrated in the last subsection to study the short-time behaviour of the critical dynamics for the Ising model and to determine the critical characteristic function for the initial magnetization. It has been pointed out in the previous letter [25], for the Potts model in the determination of  $\varphi(2, m_0)$  the finite size effect for the lattice pair  $(L_1, L_2) = (72, 144)$  is already very small. This situation is similar for the Ising

model. Therefore, in this section we restrict our discussions to the lattice pair  $(L_1, L_2) = (64, 128)$ . For the determination of  $\varphi(4, m_0)$ , we use the lattice pair  $(L_1, L_2) = (32, 128)$ . For lattice sizes  $L = 36, 72$  and  $144$ , we have performed simulations with 80 000, 32 000 and 8 000 samples of different initial configurations respectively. The initial magnetization for the lattice  $L = 128$  takes the value  $m_0 = 0.10, 0.20, 0.30, 0.40, 0.50, 0.60, 0.70, 0.80$  and  $1.00$ . For the lattice  $L = 128$  with  $m_0 \geq 0.60$ , the statistics is 16 000. The maximum evolution time is  $t = 2500$  for the lattice size  $L = 128$ ,  $t = 250$  for the lattice size  $L = 72$  and  $t = 100$  for the lattice size  $L = 36$ .

In case of the Potts model, we believe that the dynamic exponent  $z = 2.196$  used in the last subsection is very close to the true value [10, 12, 16]. However, for the Ising model the value of the dynamic exponent is still a matter of debate. Values ranging from  $z = 2.13$  to  $z = 2.17$  can be found in the literature [28, 29, 30, 18, 19, 31, 32]. Fortunately, in the determination of the critical characteristic function  $\varphi(b, m_0)$  the deviation about one percent in the value of  $z$  does not induce a big change in the results for  $\varphi(b, m_0)$ , at least for not too big  $m_0$ . In Fig. 8, a scaling plot for the magnetization of the lattice size  $L = 128$  with  $m_0 = 0.40$  and lattice size  $L = 64$  is displayed. Crosses and circles are the same data for the magnetization of  $L = 128$ , but rescaled with two different values of the dynamic exponent  $z$ ,  $z = 2.15$  and  $z = 2.17$  respectively. We can see the difference is very small. The resulting values of  $\varphi(2, m_0)$  are  $\varphi(2, 0.40) = 0.5588(25)$  for  $z = 2.15$  and  $\varphi(2, 0.40) = 0.5567(25)$  for  $z = 2.17$ . On the other hand, in our numerical measurements from the short-time dynamics the value of  $z$  tends to  $z = 2.15$  [19, 12]. Therefore, in this section we always use the value  $z = 2.15$  in the analyses of the data unless we specify other values. Later we will give some more details on this point.

Here we should also mention that as in the case of the Potts model, for the lattice pair  $(L_1, L_2) = (64, 128)$  the difference between data with and without the sharp preparation technique, i.e. the extra finite size effect from the initial configurations is already not big. For example, without the sharp preparation of the initial magnetization we get  $\varphi(2, 0.40) = 0.5566(18)$  from the scaling collapse of the magnetization. Within the statistical errors, this is consistent with  $\varphi(2, 0.40) = 0.5588(25)$  obtained with the sharp preparation technique.

In Fig. 9, a scaling plot for the magnetization of the lattice size  $L = 128$  with  $m_0 = 0.30$  and lattice size  $L = 32$  is displayed. The scaling collapse looks also very nice even though the fluctuation is slightly bigger than that in the scaling plot for the lattice pair  $(L_1, L_2) = (64, 128)$ . The resulting value of  $\varphi(2, m_0)$  is  $\varphi(4, 0.30) = 0.585(2)$ . Practically, the measurement of  $\varphi(4, m_0)$  is more difficult than that of  $\varphi(2, m_0)$ . We have to perform simulations for bigger lattice sizes and longer evolution time. Much computer time is needed. Therefore, to measure  $\varphi(b, m_0)$  for even bigger  $b$ , it is not wise to follow the way discussed in this paper.

To see the possible effect of the microscopic time scale  $t_{mic}$ , we can analyse the data also by the local fit. In Fig. 10,  $\varphi(2, m_0)$  with  $m_0 = 0.40$  obtained from

the magnetization with lattice size  $L = 128$  and  $L = 64$  is plotted versus time  $t$ . We can see clearly that  $t_{mic}$  is also very small,  $t_{mic} \leq 10$ . Therefore, in this section we always start our measurements of the critical characteristic function  $\varphi(2, m_0)$  from the time  $t = 10$ .

In case of the Potts model, when  $m_0$  is bigger the scaling collapse for the magnetization  $M(t, m_0)$  is not as good as that for the magnetization difference  $M_d(t, m_0)$ . However, it is interesting that for the Ising model both scaling plots for  $M(t, m_0)$  and  $M_d(t, m_0)$  give similar results, at least when one takes  $z = 2.15$ . This shows that in the simulations we do not get so much fluctuations from  $M(t, 1)$ . In other words, the data of  $M(t, 1)$  for the lattice pair  $(L_1, L_2)$  collapse very well. In Table 2, the function  $\varphi(2, m_0)$  and  $\varphi(4, m_0)$  obtained from a global fit of the magnetization  $M(t, m_0)$  are listed. For  $z = 2.17$ , the case is slightly different. We will discuss this later.

In Fig. 6, the final results for the effective dimension  $x(2, m_0)$  and  $x(4, m_0)$  are given. The data are taken from Table 2. Stars with solid line are of  $x(2, m_0)$  and diamonds with dashed line are of  $x(4, m_0)$ . From Fig. 6 we observe that the effective dimension  $x(b, m_0)$  for the Ising model and the Potts model is quite different. We would expect that  $x(b, m_0)$  always monotonously decreases as  $m_0$  goes from  $m_0 = 0$  to  $m_0 = 1$ . This is indeed the case for the Ising model. However, for the Potts model  $x(b, m_0)$  first increases and after some time reaches its maximum and then decreases. This is consistent with what one observes in the numerical measurement of the exponent  $\theta$  [12]. When  $m_0$  increases from  $m_0 = 0.0$ , for the Ising model the effective  $\theta$  decreases while for the Potts model it increases. This phenomenon remains to be understood. It is challenging to derive analytically the generalized dynamic scaling form in Eq.(3) and the critical characteristic function  $\varphi(b, m_0)$ .

Now, naturally one may ask, is the critical characteristic function  $\varphi(b, m_0)$  really non-trivial? In other words, it may happen that if we take another field rather than the initial magnetization as the scaling variable one exponent is sufficient to describe the scaling behaviour of the initial magnetization. *Theoretically*, this is possible. For example, we can take  $g = F^{-1}(m_0)$  as a scaling variable as it is discussed in Sec. 2. However, the problem is not so simple. First, in general we don't know the function  $F^{-1}(m_0)$ . Secondly, the physical meaning of  $g$  is not clear. Actually,  $F^{-1}(m_0)$  is just the function we intend to measure. Very recently, we have received a preprint [26] by U. Ritschel and P. Czerner (Univ. Essen, FRG) where a comment is given to the topic addressed in this paper and the previous letter [25]. It is said that if one uses the initial external magnetic field as the scaling variable rather than the initial magnetization, the exponent  $x_0$  is sufficient to describe the dynamic scaling. They got an indication for that from their data of  $x(b, m_0)$  for the Ising model. However, their conjecture apparently fails in the Potts model. For the Ising model, their data overlap partly and are consistent with ours within the errors. But our lattice sizes are bigger and our errors are smaller. Our data within errors are not consistent with their

conjecture. Actually, some points of their data are also outside of their expected values.

At high temperature, the external magnetic field  $h$  and the initial magnetization  $m_0$  have a simple relation, for the Ising model [26]

$$m_0 = \tanh(h), \quad (12)$$

and for the Potts model

$$m_0 = \frac{3}{2} \left( \frac{e^h}{e^h + 2} - \frac{1}{3} \right). \quad (13)$$

Supposing  $h$  is used as a scaling variable in the scaling form in Eq.(3), the effective anomalous dimension  $y(b, m_0)$  of  $h$  can also be extracted from the numerical data. In the limit  $m_0 = 0.0$ ,  $y(b, 0) = x(b, 0) = x_0$ . The exponent  $x_0$ , which has been measured in Ref. [10, 12], is  $x_0 = 0.536$  and  $x_0 = 0.298$  for both the Ising and the Potts model respectively. The results are shown in Fig. 11. For the Potts model,  $y(b, m_0)$  apparently is not a constant. For the Ising model, it is not too far from a constant but there is significant difference. Especially, as is pointed out before, the results obtained from both  $M_d(t, m_0)$  and  $M(t, m_0)$  agree very well. For  $m_0 \geq 0.80$ , the fluctuations for the Potts model become very big. We can not see whether  $y(2, m_0)$  continues to increase or starts to decrease. For the Ising model, the data are not available.

We have discussed that the dynamic exponent  $z$  is not known so rigorously. Therefore we may also present the results with other values of  $z$ . For example, if one takes  $z = 2.17$  for the Ising model, the resulting  $y(2, m_0)$  is displayed in Fig. 12. Stars are of  $y(2, m_0)$  measured from  $M(t, m_0)$  and squares are that from  $M_d(t, m_0)$ . The results obtained from  $M_d(t, m_0)$  coincide very well with those measured with  $z = 2.15$  (the solid line). However, for relative bigger  $m_0$  the data from  $M(t, m_0)$  show some deviation. We believe the result of  $M_d(t, m_0)$  are nearer to the true values of  $y(2, m_0)$ . In the scaling plot for  $M(t, m_0)$  one may have got some errors from  $M(t, 1)$ . This might also indicate that  $z = 2.15$  is a better value for the dynamic exponent  $z$  of the Ising model. Anyhow, even the data from  $M(t, m_0)$  are not compatible with a constant.

## 4 Conclusions and remarks

We have numerically simulated the universal short-time behaviour of the dynamic relaxation process for the two dimensional Ising and the Potts model at criticality starting from an initial state with very high temperature and *arbitrary* magnetization. The critical characteristic function for the initial magnetization, which is introduced to describe the generalized dynamic scaling, is determined with finite size scaling. It is interesting that the critical characteristic functions for the Ising and the Potts model look quite different. When the initial magnetization varies from  $m_0 = 0$  to  $m_0 = 1$ , the effective dimension of the initial magnetization

for the Ising model monotonously decreases, while that for the Potts model first rises and then decreases. It is challenging to derive analytically the generalized scaling form as well as the critical characteristic function  $\varphi(b, m_0)$ . However, the standard perturbative renormalization group methods for the continuum models, as e.g. the  $\phi^4$ -theory, do not apply here.

The initial magnetization can be considered as a coupling of the systems. The generalized scaling form describes the crossover scaling behaviour of the dynamic systems between the fixed point  $m_0 = 0$  to  $m_0 = 1$ . This kind of phenomena can be found in many statistical systems, for example, at the ordinary phase transition in the surface critical phenomena. When a non-zero magnetization is applied to the surface, a similar scenario as in the short-time dynamics appears.

*Acknowledgement:* The author would like to thank L. Schülke for helpful discussions.

## References

- [1] H. K. Janssen, B. Schaub and B. Schmittmann, Z. Phys. **B 73** (1989) 539.
- [2] H. K. Janssen, in *From Phase Transition to Chaos*, edited by G. Györgyi, I. Kondor, L. Sasvári and T. Tél, Topics in Modern Statistical Physics (World Scientific, Singapore, 1992).
- [3] K. Oerding and H. K. Janssen, J. Phys. A: Math. Gen. **26** (1993) 3369,5295.
- [4] K. Oerding and H. K. Janssen, J. Phys. A: Math. Gen. **27** (1994) 715.
- [5] H. W. Diehl and U. Ritschel, J. Stat. Phys. **73** (1993) 1.
- [6] U. Ritschel and H. W. Diehl, Nucl. Phys. **B 464** (1996) 512.
- [7] D. A. Huse, Phys. Rev. **B 40** (1989) 304.
- [8] K. Humayun and A. J. Bray, J. Phys. A **24** (1991) 1915.
- [9] Z.B. Li, U. Ritschel and B. Zheng, J. Phys. A: Math. Gen. **27** (1994) L837.
- [10] L. Schülke and B. Zheng, Phys. Lett. **A 204** (1995) 295.
- [11] N. Menyhárd, J. Phys. A: Math. Gen. **27** (1994) 663.
- [12] K. Okano, L. Schülke, K. Yamagishi and B. Zheng, Nucl. Phys. **B 485** (1997) 727.
- [13] P. Czerner and U. Ritschel, Phys. Rev. **E 53** (1996) 3333.
- [14] K. Okano, L. Schülke, K. Yamagishi and B. Zheng, *Monte Carlo simulation of the short-time behaviour of the dynamic XY model*, Siegen Univ., 1997, preprint SI-97-02.
- [15] Z.B. Li, X.W. Liu, L. Schülke and B. Zheng, Physica A (1997) , to be published.

- [16] L. Schülke and B. Zheng, Phys. Lett **A** **215** (1996) 81.
- [17] L. Schülke and B. Zheng, in *Proceeding of the XIVth International Symposium on Lattice Field Theory*, Vol. 53 of *Nucl. Phys. B (Proc. Suppl.)*, edited by C. Bernhard, M. Golterman, M. Ogilvie and J. Potvin (North Holland Publishing Co., Amsterdam, 1997), pp. 712–714.
- [18] Z.B. Li, L. Schülke and B. Zheng, Phys. Rev. Lett. **74** (1995) 3396.
- [19] Z.B. Li, L. Schülke and B. Zheng, Phys. Rev. **E** **53** (1996) 2940.
- [20] L. Schülke and B. Zheng, *Monte Carlo Measurement of the Global Persistence Exponent*, Siegen Univ., preprint, SI-97-03, 1997.
- [21] X.W. Liu and Z.B. Li, *The universality of dynamic exponent  $\theta'$  demonstrated by the dynamical two-dimensional Ising model*, Zhongshan Univ., preprint, 1995.
- [22] U. Ritschel and P. Czerner, *Microscopic non-universality versus macroscopic universality in algorithms for critical dynamics*, Univ. of Essen, preprint, 1996.
- [23] S.N. Majumdar, A.J. Bray, S. Cornell and C. Sir, Phys. Rev. Lett. **77** (1996) 3704.
- [24] S.N. Majumdar, C. Sir, A.J. Bray and S. Cornell, Phys. Rev. Lett. **77** (1996) 2867.
- [25] B. Zheng, Phys. Rev. Lett. **77** (1996) 679.
- [26] U. Ritschel and P. Czerner, Univ. of Essen, preprint, 1996.
- [27] U. Ritschel and P. Czerner, Phys. Rev. Lett. **75** (1995) 3882.
- [28] S. Tang and D. P. Landau, Phys. Rev. **B** **36** (1987) 567.
- [29] D. P. Landau, S. Tang and S. Wansleben., Journal de Physique Colloque **49** (1988) C8.
- [30] N. Ito, Physica **A** **196** (1993) 591.
- [31] P. Grassberger, Physica **A** **214** (1995) 547.
- [32] M.P. Nightingale and H.W.J. Blöte , Phys. Rev. Lett. **76** (1996) 4548.

$m_0$	$\chi(2, m_0)$	$\chi(4, m_0)$
0.14	0.1800(04)	0.233(1)
0.22	0.2866(10)	0.378(2)
0.30	0.3952(11)	0.521(3)
0.40	0.5299(07)	0.691(4)
0.50	0.6586(31)	0.815(8)
0.60	0.7678(23)	0.907(6)
0.70	0.8657(29)	0.954(3)
0.80	0.9272(91)	0.987(7)

Table 1: The characteristic function  $\varphi(b, m_0)$  for the Potts model measured from the magnetization difference  $M_d(t)$ .

$m_0$	$\varphi(2, m_0)$	$\varphi(4, m_0)$
0.10	0.1439(04)	0.206(01)
0.20	0.2857(14)	0.405(03)
0.30	0.4254(10)	0.585(02)
0.40	0.5588(25)	0.741(07)
0.50	0.6800(31)	0.847(13)
0.60	0.7890(38)	0.931(13)
0.70	0.8783(78)	0.964(12)

Table 2: The characteristic function  $\varphi(b, m_0)$  for the Ising model measured from the magnetization.

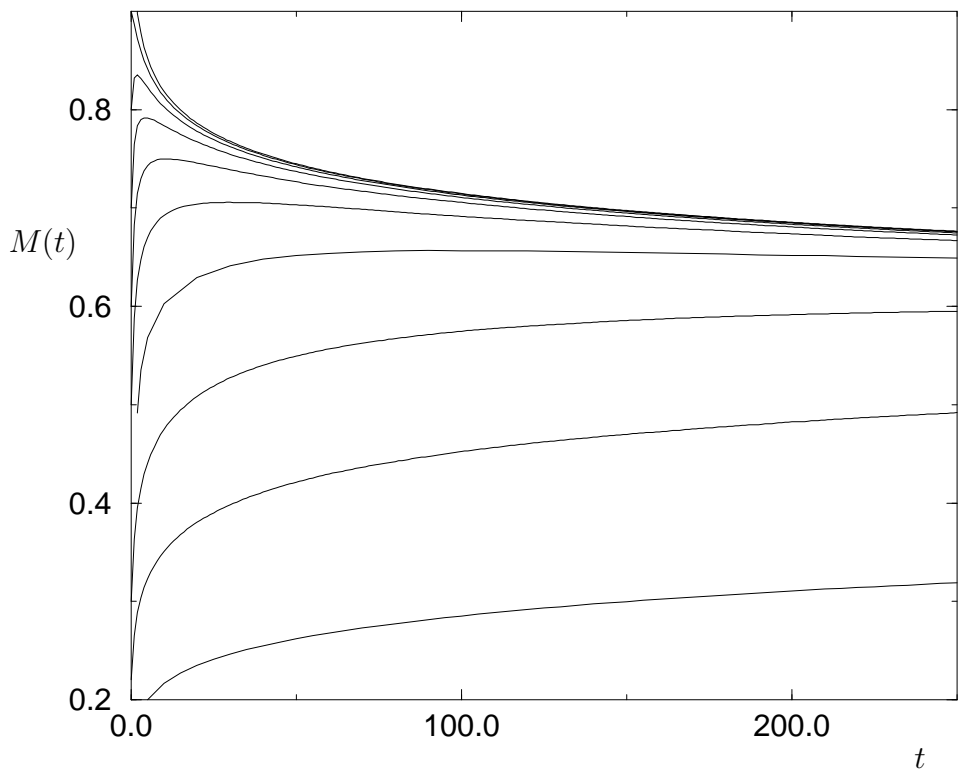


Figure 1: Magnetization profiles for the Potts model with  $L = 72$  and  $m_0 = 0.14, 0.22, 0.30, 0.40, 0.50, 0.60, 0.70, 0.80, 0.90$  and  $1.00$ .

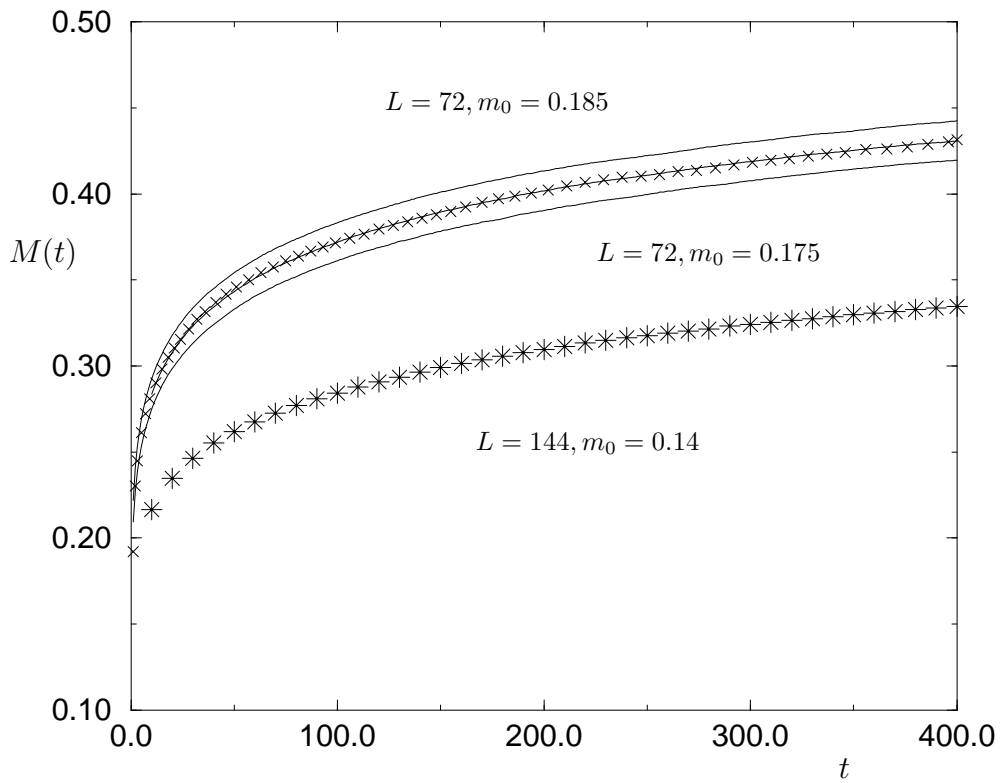


Figure 2a: The scaling plot for the magnetization with  $(L_1, L_2) = (72, 144)$  for the Potts model. For the lattice size  $L_2 = 144$ , the initial magnetization  $m_0 = 0.14$ .

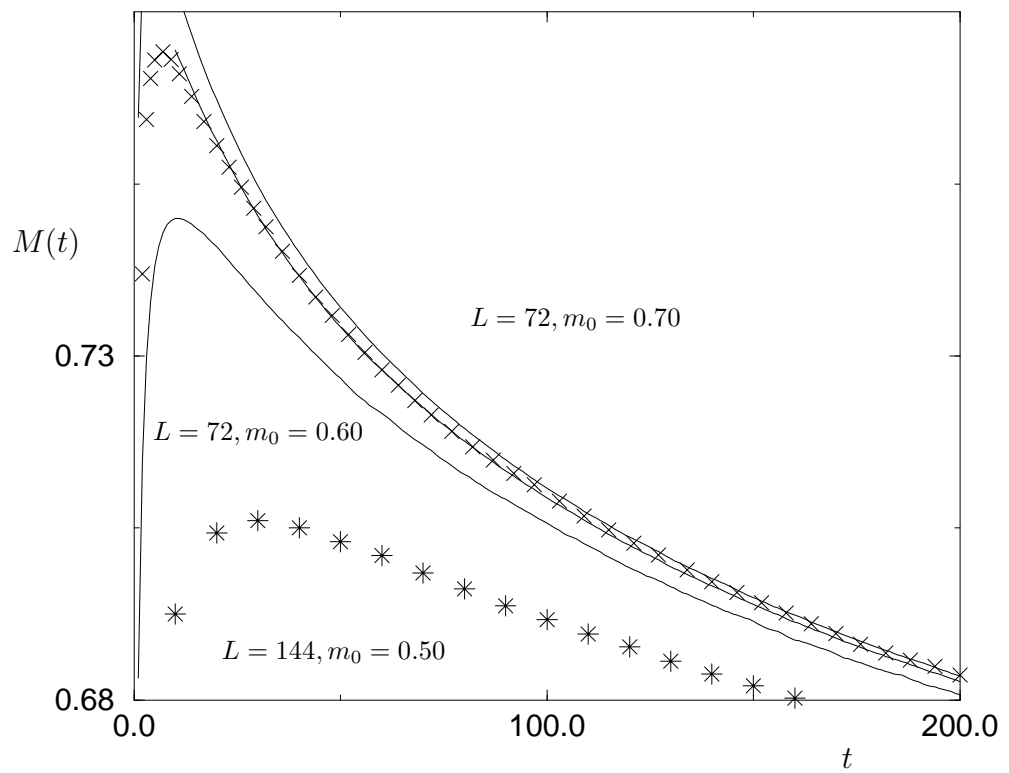


Figure 2b: The scaling plot for the magnetization with  $(L_1, L_2) = (72, 144)$  for the Potts model. For the lattice size  $L_2 = 144$ , the initial magnetization  $m_0 = 0.50$ .

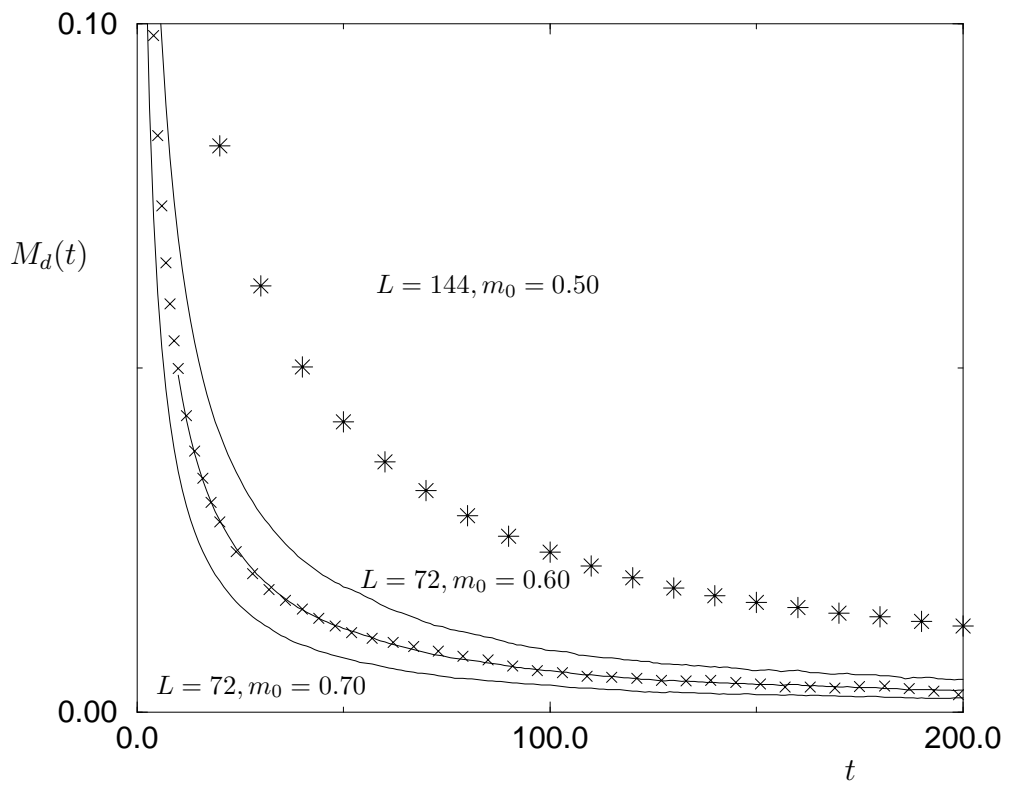


Figure 3: The scaling plot for the magnetization difference  $M_d(t)$  with  $(L_1, L_2) = (72, 144)$  for the Potts model. For the lattice size  $L_2 = 144$ , the initial magnetization  $m_0 = 0.50$ .

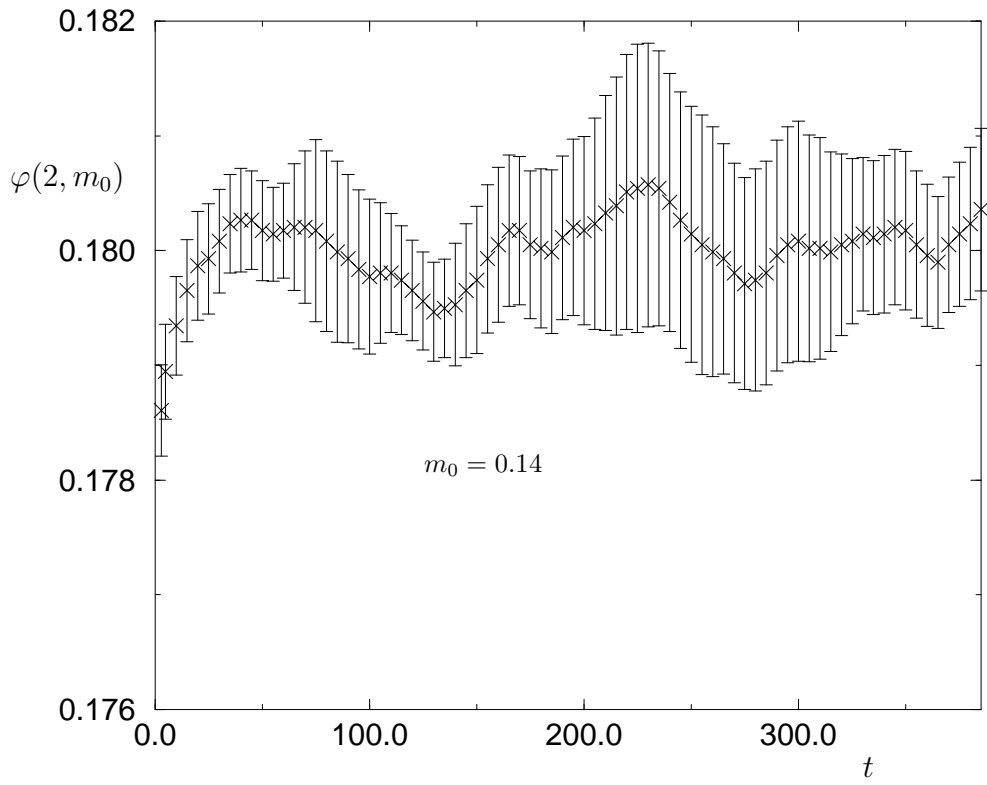


Figure 4a: The characteristic function  $\varphi(2, m_0)$  estimated with  $(L_1, L_2) = (72, 144)$  from a 'local' fit of  $M_d(t)$  for the Potts model. For the lattice size  $L_2 = 144$ , the initial magnetization  $m_0 = 0.14$ .

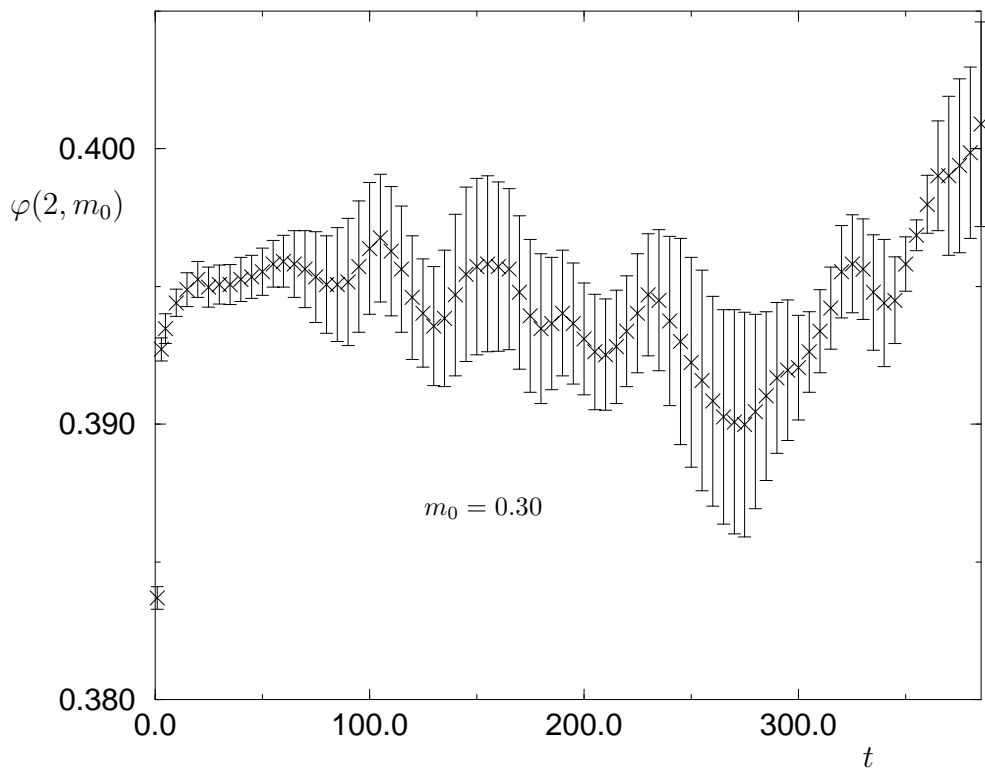


Figure 4b: The characteristic function  $\varphi(2, m_0)$  estimated with  $(L_1, L_2) = (72, 144)$  from a 'local' fit of  $M_d(t)$  for the Potts model. For the lattice size  $L_2 = 144$ , the initial magnetization  $m_0 = 0.30$ .

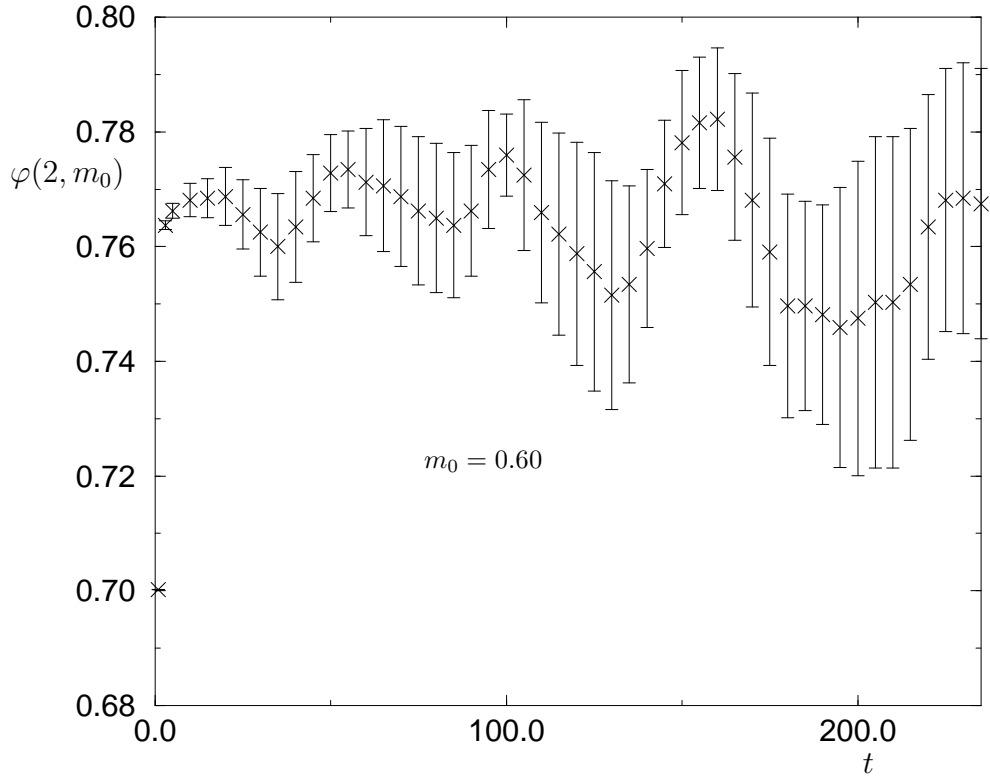


Figure 4c: The characteristic function  $\varphi(2, m_0)$  estimated with  $(L_1, L_2) = (72, 144)$  from a 'local' fit of  $M_d(t)$  for the Potts model. For the lattice size  $L_2 = 144$ , the initial magnetization  $m_0 = 0.60$ .

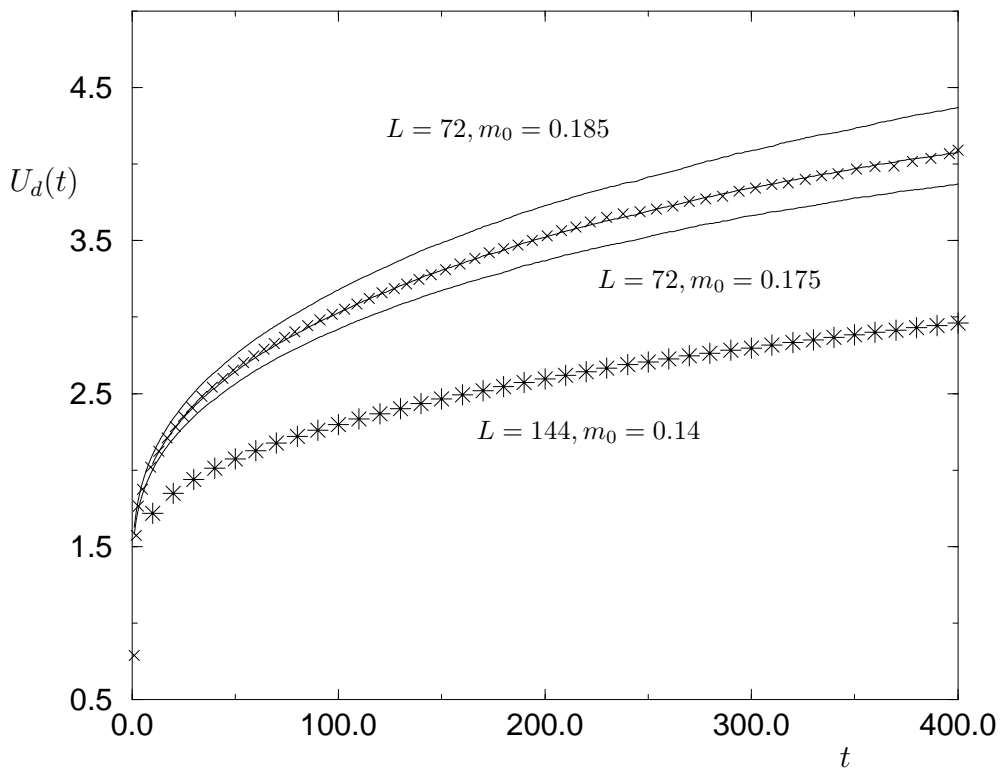


Figure 5: The scaling plot for the Binder-type cumulant  $U_d(t, m_0)$  with  $(L_1, L_2) = (72, 144)$  for the Potts model. For the lattice size  $L_2 = 144$ , the initial magnetization  $m_0 = 0.14$ .

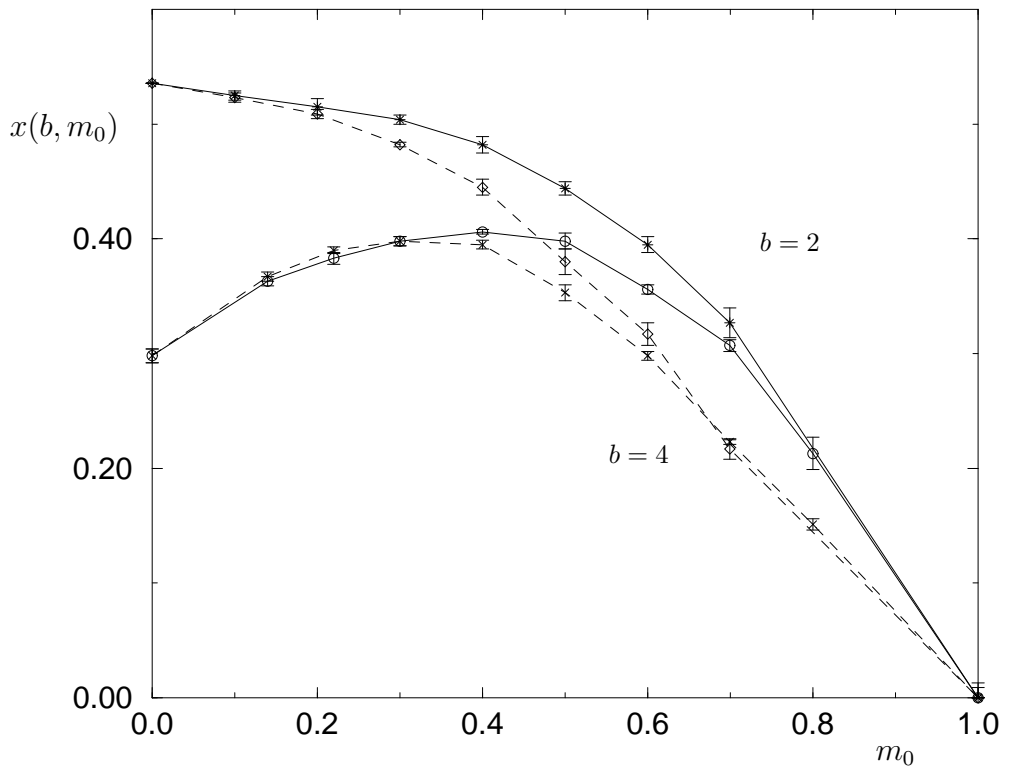


Figure 6: The effective dimension  $x(b, m_0)$  for both the Ising and the Potts model. For the Potts model the data are obtained from the magnetization difference  $M_d(t, m_0)$  with  $(L_1, L_2) = (72, 144)$  and  $(36, 144)$ . Circles with solid line are of  $x(2, m_0)$  and crosses with dashed line are of  $x(4, m_0)$ . For the Ising model results are obtained from the magnetization  $M(t, m_0)$  with  $(L_1, L_2) = (64, 128)$  and  $(32, 128)$ . Stars with solid line are of  $x(2, m_0)$  and diamonds with dashed line are of  $x(4, m_0)$ .

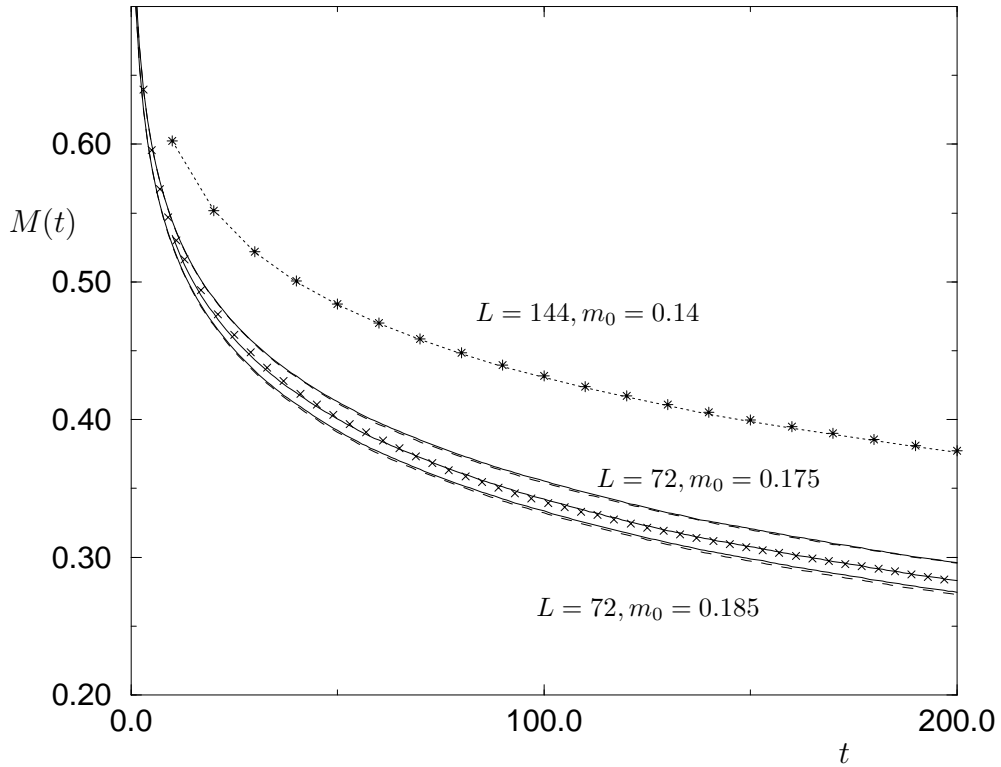


Figure 7: The scaling plot for the magnetization difference  $M_d(t)$  with  $(L_1, L_2) = (72, 144)$  for the Potts model. For the lattice size  $L_2 = 144$ , the initial magnetization  $m_0 = 0.14$ . The sharp preparation technique is not adopted. For comparison, the corresponding magnetization difference profiles with the sharp preparation technique are also displayed for the lattice sizes  $L = 144$  and  $L = 72$  with the dotted line and the dashed lines respectively.

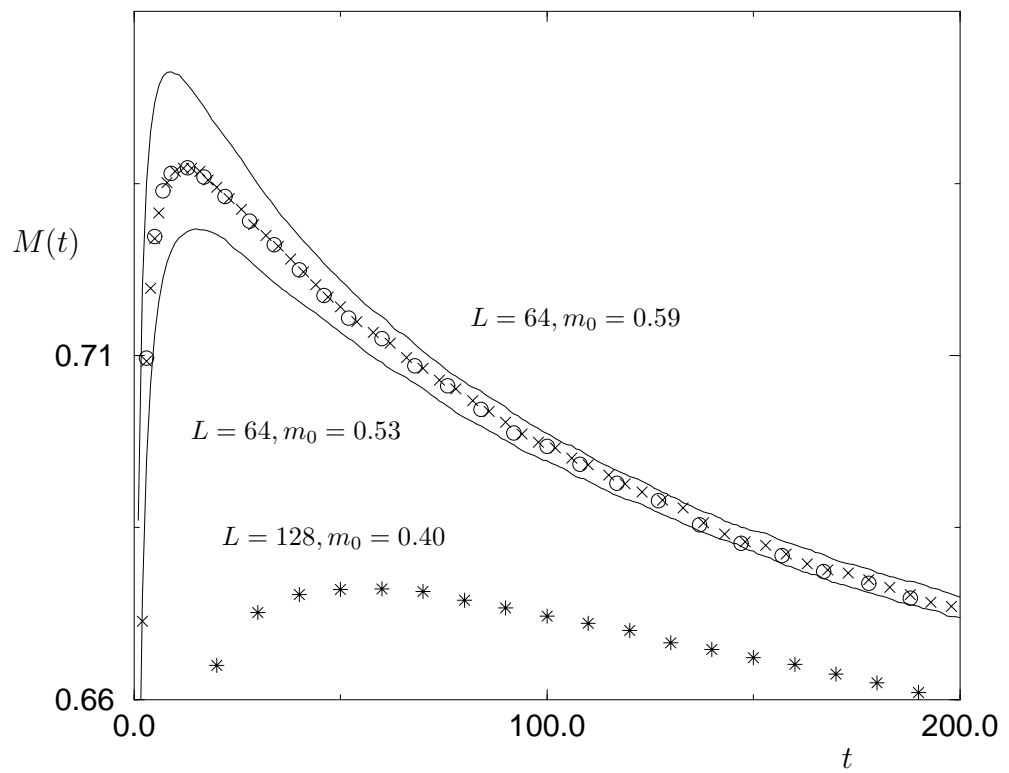


Figure 8: The scaling plot for the magnetization with  $(L_1, L_2) = (64, 128)$  for the Ising model. Crosses correspond to  $z = 2.15$  and circles are from  $z = 2.17$ .

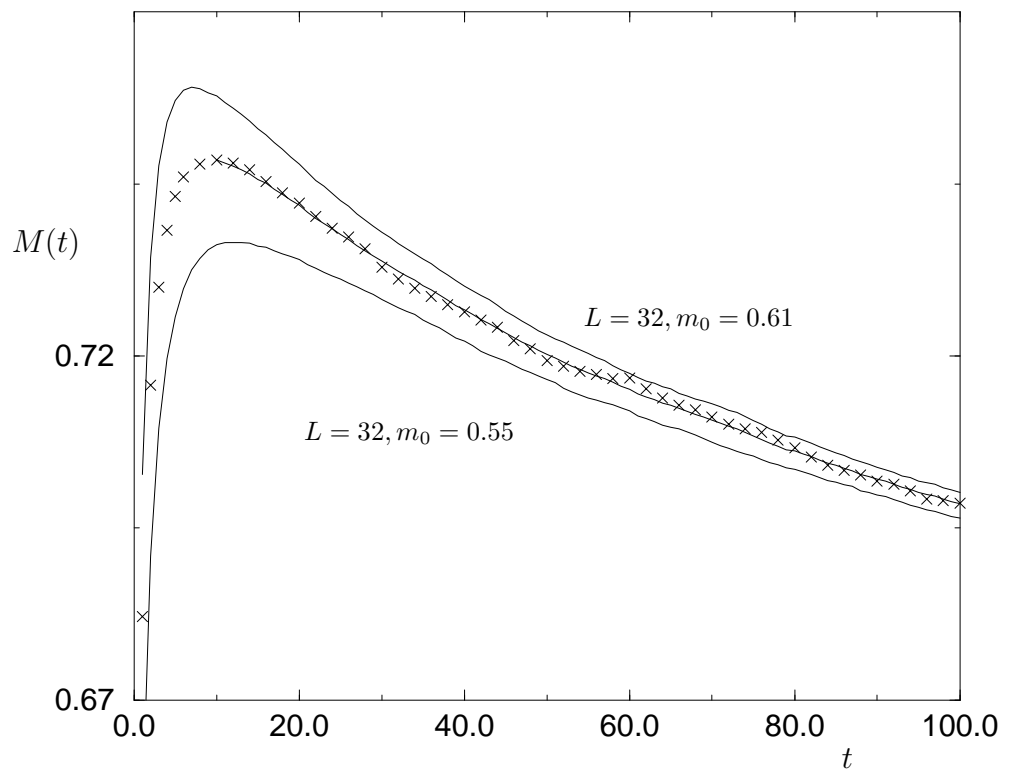


Figure 9: The scaling plot for the magnetization with  $(L_1, L_2) = (32, 128)$  for the Ising model. Crosses are for the rescaled magnetization for  $L = 128$  with  $m_0 = 0.30$ .

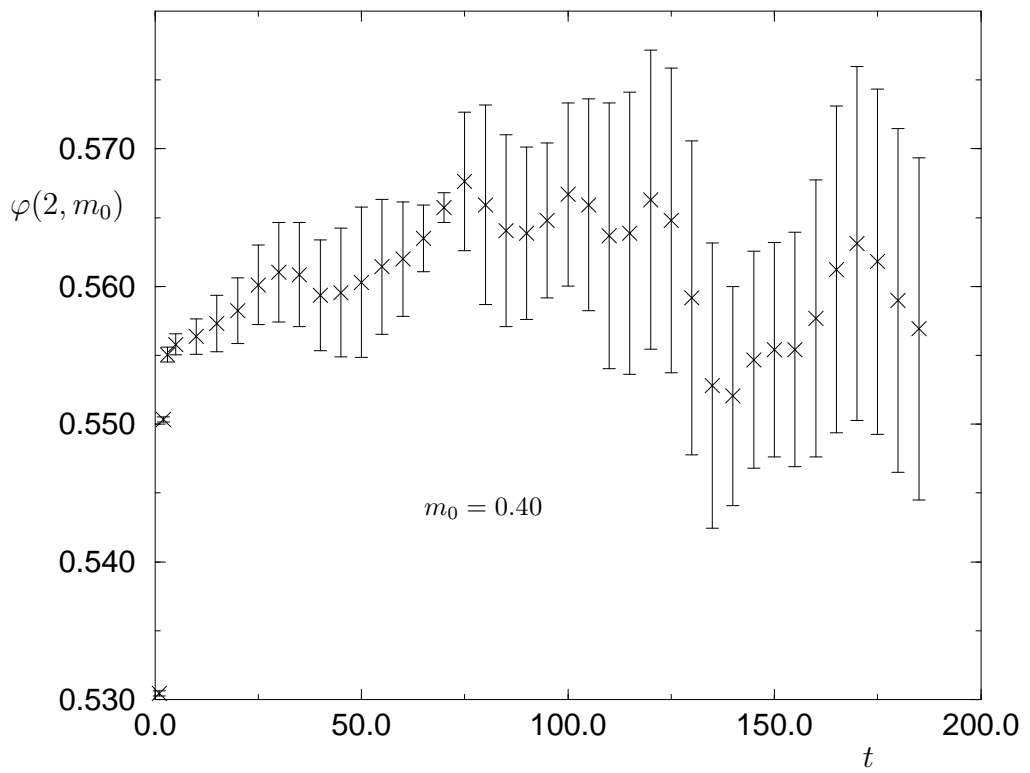


Figure 10: The characteristic function  $\varphi(2, m_0)$  estimated with  $(L_1, L_2) = (64, 128)$  from a 'local' fit of  $M(t)$  for the Ising model. For the lattice size  $L_2 = 128$ , the initial magnetization  $m_0 = 0.40$ .

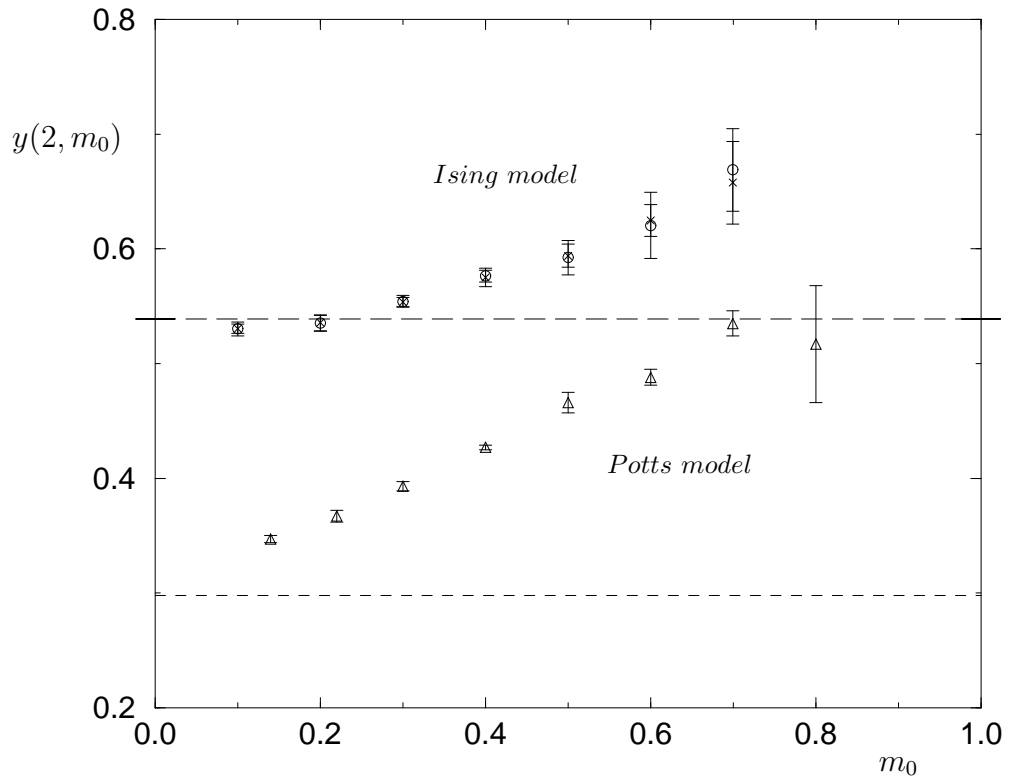


Figure 11: The effective dimension  $y(2, m_0)$  for both the Ising and the Potts model. The long dashed and dashed line are the exponent  $x_0$  for the Ising and the Potts model respectively, measured in the limit  $m_0 = 0.0$ . Crosses are of  $y(2, m_0)$  for the Ising model calculated from Table 2 and circles are the same but obtained from the scaling plot of  $M_d(t, m_0)$ . Triangles are of  $y(2, m_0)$  for the Potts model obtained from Table 1.

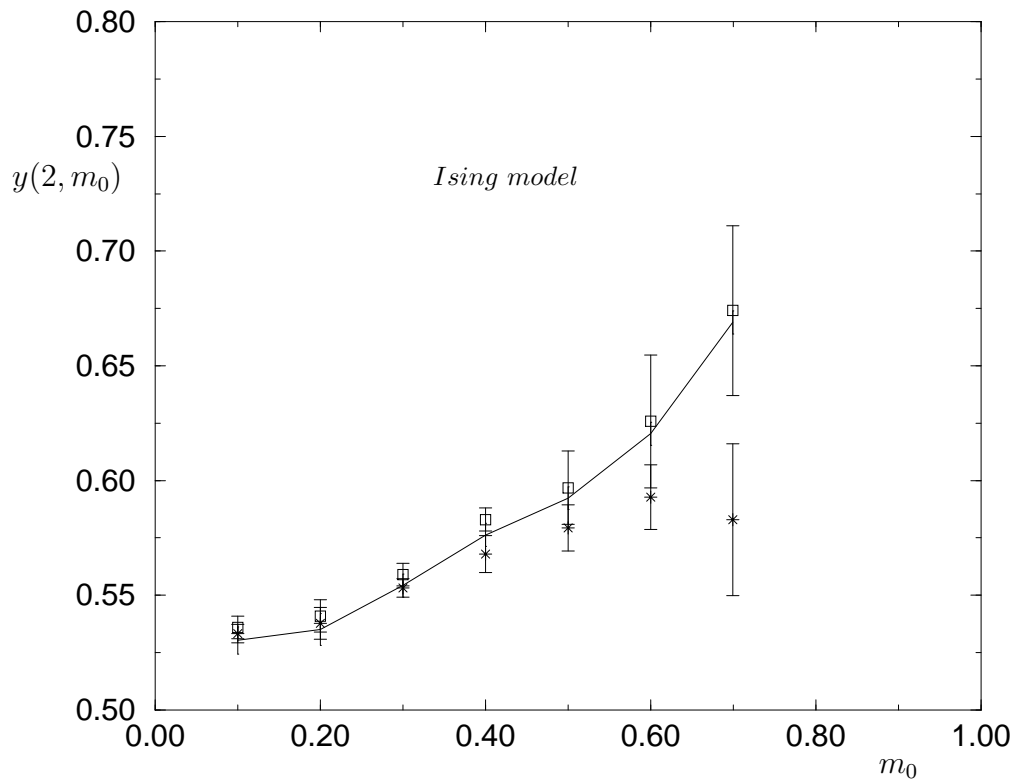


Figure 12: The effective dimension  $y(2, m_0)$  for the Ising model with  $z = 2.17$ . The long dashed line is the exponent  $x_0$  for the Ising model. Stars are of  $y(2, m_0)$  calculated from  $M(t, m_0)$  and the squares are the same but obtained from the scaling plot of  $M_d(t, m_0)$ . The solid line is that estimated from  $M_d(t, m_0)$  but with  $z = 2.15$ .